Dendritic Poly(benzyl ether)-*b*-poly(*N*-vinylcaprolactam) Block Copolymers: Self-Organization in Aqueous Media, Thermoresponsiveness and Biocompatibility

Gang Tang, Minqi Hu, Fuxi He, Dan You, Yangyang Qian, Yunmei Bi

College of Chemistry and Chemical Engineering, Yunnan Normal University, Kunming 650500, People's Republic of China
Correspondence to: Y. Bi (E-mail: yunmeibi@hotmail.com)

Received 1 September 2017; accepted 18 October 2017; published online 00 Month 2017
DOI: 10.1002/pola.28897

ABSTRACT: Four generations of new amphiphilic thermoresponsive linear-dendritic block copolymers (LDBCs) with a linear poly(*N*-vinylcaprolactam) (PNVCL) block and a dendritic poly(benzyl ether) block are synthesized by atom transfer radical polymerization (ATRP) of *N*-vinylcaprolactam (NVCL) using dendritic poly(benzyl ether) chlorides as initiators. The copolymers have been characterized by ^{1}H NMR, FTIR, and GPC showing controlled molecular weight and narrow molecular weight distribution (PDI $\leq$ 1.25). Their self-organization in aqueous media and thermoresponsive property are highly dependent on the generation of dendritic poly(benzyl ether) block. It is observed for the LDBCs that the self-assembled morphology changes from irregularly spherical micelles, vesicles, rod-like large compound vesicles (LCVs), to the coexistence of spherical micelles and rod-like LCVs, as the generation of the dendritic poly(benzyl ether) increases. The results of a cytotoxicity study using an MTT assay method with L929 cells show that the LDBCs are biocompatible. © 2017 Wiley Periodicals, Inc. J. Polym. Sci., Part A: Polym. Chem. **2017**, *00*, 000–000

KEYWORDS: biocompatibility; linear-dendritic block copolymers; poly(*N*-vinylcaprolactam); self-assembly; synthesis; thermoresponsiveness

INTRODUCTION Linear-dendritic block copolymers (LDBCs), which combine the easy synthesis, availability, and processability of linear polymeric chains with the regular and well-defined dendritic segments, are particularly attractive due to their multicomponent constitutions, unique self-assembly properties, and multivalent characteristics.[1–3] Importantly, the solution and solid state properties of the LDBCs can be tuned by adjusting the length of the linear chains, generation number of the dendron, and the chemical structure/polarity of both blocks. Amphiphilic LDBCs, as a special type of LDBCs, can self-assemble into various supramolecular structures in aqueous solution, which exhibit excellent loading capacity for hydrophobic small molecules medicine, since most drug molecules are hydrophobic and therefore can be useful in drug delivery.[4–12] In particular, if stimulus-sensitive moieties are incorporated into the chemical structure of the amphiphilic LDBCs, the resulting polymeric aggregates may have a controlled and programmed response to an external stimulus.[13] Along with all possible stimuli, temperature is an especially attractive one because the corresponding functional moieties are comparatively easy to be introduced and fabricated.

Over the past decades, thermoresponsive polymers have been extensively investigated due to their promising applications in drug delivery, nanotechnology, and tissue engineering.[14–18] When an aqueous solution of a thermoresponsive polymer is heated above its lower critical solution temperature (LCST), a macroscopic phase separation occurs. Poly(*N*-vinylcaprolactam) (PNVCL) is regarded as second only to poly(*N*-isopropylacrylamide) (PNIPAM) the most popular thermoresponsive polymer.[19–21] PNVCL has a LCST in aqueous solution at temperatures close to physiological temperatures. Apart from that, PNVCL is nonionic, nontoxic, and biocompatible. In comparison with other studied thermoresponsive polymers, PNVCL is not able to form hydrogen bonds due to the lack of a H-donor in the molecular structure (unlike, e.g., PNIMAM), which results in lower interaction with biomolecules, higher expected bioacceptability, and no tendency to crystallization, which may cause poly(2-isopropyl-2-oxazoline) to phase separate partly irreversibly. It is also not poly(ethyleneoxide)-based, which would result in formation anti-PEO antibodies.[22–25] These make PNVCL more suitable for biomedical applications.[26]

The linearly PNVCL-based block copolymers have gained much impetus in recent years due to the enhanced boost of the so-called controlled free radical polymerization methods, such as atom transfer free radical polymerization

Additional Supporting Information may be found in the online version of this article.

(ATRP),[27–29] reversible addition fragmentation chain transfer (RAFT) polymerization,[30–34] or organometallic-mediated radical polymerization.[35–37] However, only six recent articles were concerned on nonlinear block copolymers containing the PNVCL moiety.[38–43] Recently, star-shaped copolymers with four and six poly(ε-caprolactone)-block-poly(*N*-vinylcaprolactam) S(PCL-*b*-PNVCL) arms were successfully synthesized by combining ring opening polymerization of ε-caprolactone (CL) and RAFT polymerization of *N*-vinylcaprolactam (NVCL).[39] Hyperbranched polycaprolactone-*click*-poly(*N*-vinylcaprolactam) amphiphilic copolymers was synthesized.[40] We have reported the first preparation of thermoresponsive LDBCs composed PNVCL and dendritic aromatic polyamides of two different generations via the RAFT technique, employing dendritic chain-transfer agents possessing a single dithiocarbamate moiety at the focal point.[41] However, the studies on the self-assembly behavior of higher generations than [G-2] of PNVCL-based LDBCs still remain largely unexplored.

In general, the synthesis methods for LDBCs include (i) the coupling method: coupling of a previously synthesized dendron and a monofunctional or oligofunctional linear polymer chain; (ii) the "chain-first" method: one or two dendrons are radially grown from a linear polymer; (iii) the "dendron-first" method: a linear polymer is polymerized from the focal points of a dendron.[1,10] A facile strategy for preparing well-defined LDBCs is the use of dendrons as macromolecular initiators for the controlled free radical polymerization of vinyl monomers. This strategy was pioneered by Fréchet and Gitsov.[44–46] The dendron-first approach has proven to be very useful for the preparation of poly(benzyl ether) based LDBCs.[1]

Generally, controlling the morphology of self-assembled aggregates of LDBCs, through the tuning of generation number of dendritic segment, is of great importance to their related properties and practical applications.[47–50] It has been reported that some dendrimers display generation-dependent cytotoxicity.[51,52] In this study, a new series of thermoresponsive amphiphilic linear-dendritic block copolymers (LDBCs) based on PNVCL as a hydrophilic linear block and four generations of dendritic poly(benzyl ether) as a hydrophobic block were synthesized by growing a PNVCL linear arm from the focal point of poly(benzyl ether) dendrons via ATRP. The effect of the generation number of the dendritic block and the concentrations of the LDBCs solutions on the thermoresponsive properties and micellar characteristics of these LDBCs in an aqueous phase were investigated. The cytotoxicity of the LDBCs *in vitro* was also evaluated for potential biomedical application.

EXPERIMENTAL

Materials

N-vinyl caprolactam (NVCL, 98%, Sigma) was distilled under reduced pressure to remove the inhibitor and restored at 4 °C. CuCl were purified by stirring in acetic acid, washed with ethanol, and then died in vacuum. 5, 5, 7, 12, 12, 14-hexamethyl-1, 4, 8, 11-tetra-azacyclotetradecane (Me_6Cyclam) was prepared according to literature method.[53] 1,4-Dioxane was refluxed on sodium and distilled from sodium benzophenone. 3,5-Dihydroxybenzyl alcohol was synthesized according to the method previously reported.[54] Isopropanol was used as received.

Characterizations

^{1}H NMR spectra were recorded on a Bruker DRX-500 spectrometer with $CDCl_3$ or D_2O as the solvent. The chemical shifts were calculated relative to TMS. FT-IR spectra were obtained on a Nicolet AVATAR 360 FT-IR spectrometer. Molecular weights and molecular weight distributions were determined using a Waters 2690D gel permeation chromatograph equipped a 2410 refractive index detector, Waters Styragel HR1 THF and HR2 THF columns with THF as eluent at 40 °C and a flow rate of 0.3 Ml min^{-1}. The molecular weights were calibrated against polystyrene (PS) standards. DLS measurements were performed with a Zetasizer ZEN 3600 instrument (Malvern, UK) operating at 25–45 °C using a light scattering apparatus equipped with a He-Ne laser. The scattering angle was kept at 173° (backscattering) and the wave length in the vacuum was set as 633 nm during the whole experiment. Malvern DTS 6.20 software was used to analyze the data. Each reported measurement was the average of three runs. Transmission electron microscopy (TEM) experiments were carried out on a Hitachi H-600 instrument operating at an acceleration voltage of 80 kV.

Synthesis of Dendritic Benzyl Alcohols (G_n-OH)

Dendritic benzyl alcohols (G_n-OH) was synthesized according to the previously published literature[54,55] with modification.

Synthesis of G_1-OH

K_2CO_3 (13.8 g) was dissolved in 100 mL of DMF and stirred under nitrogen for 1 h. 3,5-Dihydroxy benzyl alcohol (5.6 g, 40 mmol) was added. Then benzoyl chloride (6.8 mL, 58.6 mmol) was added dropwise to the solution at 65 °C and stirred for 4 h. The reaction mixture was then poured into ice-cooled water and the precipitate was collected by filtration. Crude mixture was purified by a silica column (petroleum ether/EtOAc, v/v = 1.5:1) and the product was obtained as white solid in 90% yield.

^{1}H NMR (500 MHz, $CDCl_3$, δ): 4.62 (d, J = 6.0 Hz, 2H; CH_2O), 5.04 (s, 4H, $PhCH_2O$), 6.55 (t, J = 2.1 Hz, 1H; CH), 6.63 (d, J = 2.1 Hz, 2H; CH), 7.25–7.43 (m, 10H, Ar H).

Synthesis of G_2-OH

G_2-OH was synthesized by the same general procedure described for the synthesis of G_1-OH. From G_1-Cl (1.69 g, 5 mmol), 3,5-dihydroxy benzyl alcohol (0.28 g, 2 mmol), 1.38 g K_2CO_3 and DMF (10 mL) were obtained 1.34 g (90%) as a white solid.

^{1}H NMR (500 MHz, $CDCl_3$, δ): 4.65 (d, J = 5.7 Hz, 2H; CH_2O), 5.00 (s, 4H, $PhCH_2O$), 5.06 (s, 8H, $PhCH_2O$), 6.54 (t, J = 2.1 Hz, 1H; CH), 6.59 (t, J = 2.4 Hz, 2H; CH), 6.63 (d, J = 2.1 Hz,

4H; CH) 6.70 (d, $J = 2.1$ Hz, 4H; CH), 7.33–7.45 (m, 20H, Ar H).

Synthesis of G_3-OH

G_3-OH was synthesized by the same general procedure described for the synthesis of G_1-OH. From G_2-Cl (3.81 g, 5 mmol), 3, 5-dihydroxy benzyl alcohol (0.28 g, 2 mmol), K_2CO_3 (1.5 g), and DMF (10 mL) were obtained 3.3 g (81%) as a white solid.

^{1}H NMR (500 MHz, $CDCl_3$, δ): 4.57 (d, $J = 6.0$ Hz, 2H; CH_2O), 4.95 (s, 8H, $PhCH_2O$), 5.01 (s, 16H, $PhCH_2O$), 6.52 (m, 3H, CH), 6.55 (d, $J = 1.8$ Hz, 2H; CH), 6.64 (d, $J = 2.1$ Hz, 4H; CH), 6.66 (d, $J = 2.1$ Hz, 4H; CH), 7.27–7.40 (m, 40H, Ar H).

Synthesis of G_4-OH

G_4-OH was synthesized by the same general procedure described for the synthesis of G_1-OH. From G_3-Cl (0.41 g, 0.25 mmol), 3,5-dihydroxy benzyl alcohol (0.41 g, 0.25 mmol), K_2CO_3 (1.5 g), and DMF (10 mL) were obtained 0.42 g (76.5%) as a white solid.

^{1}H NMR (500 MHz, $CDCl_3$, δ): 4.60 (d, $J = 5.7$ Hz, 2H; CH_2O), 4.98 (s, 28H, $PhCH_2O$), 5.04 (s, 32H, $PhCH_2O$), 6.55–6.69 (m, 42H, CH), and 7.33–7.43 (m, 80H, Ar H).

Synthesis of Dendritic Benzyl Chlorides (G_n-Cl)

Synthesis of G_1-Cl

To a solution of $SOCl_2$ (0.5 mL, 6.92 mmol) in NMP (2mL) was added the appropriate dendritic benzyl alcohol (1.00 equiv) at 0 °C under nitrogen, and stirred for 10 min at that temperature. K_2CO_3 (6.96 g, 50.35 mmol) was added and stirred for 1 h at room temperature. Then, DI water was added to dissolve K_2CO_3. The resulting solution was extracted with CH_2CI_2 (3×); the combined extracts were dried over $MgSO_4$. After the solvent had evaporated, the remaining product was purified by silica gel column chromatography (petroleum ether/EtOAc, v/v = 1.5:1) to yield a white solid. The yield was 95% (2.03 g).

^{1}H NMR (500 MHz, $CDCl_3$, δ): 4.54 (s, 2H, CH_2Cl), 5.06 (s, 4H, $PhCH_2O$), 6.60 (t, $J = 2.1$ Hz, 1H; CH), 6.67 (d, $J = 2.1$ Hz, 2H; CH), 7.28–7.41 (m, 10H, Ar H).

Synthesis of G_2-Cl

G_2-Cl was synthesized by the same general procedure described for the synthesis of G_1-Cl. From G_2-OH (2.34 g, 3.15 mmol), $SOCl_2$ (0.25 mL, 3.5 mmol), NVP (2 mL) were obtained 2.1 g (90%) as a white solid.

^{1}H NMR (500 MHz, $CDCl_3$, δ): 4.50 (s, 2H, CH_2Cl), 5.96 (s, 4H, $PhCH_2O$), 5.03 (s, 8H, $PhCH_2O$), 6.53 (t, $J = 2.1$ Hz, 1H; CH), 6.57 (t, $J = 2.4$ Hz, 2H; CH), 6.62 (d, $J = 2.1$ Hz, 4H; CH) 6.67 (d, $J = 2.1$ Hz, 4H; CH), 7.33–7.45 (m, 20H, Ar H).

Synthesis of G_3-Cl

G_3-Cl was synthesized by the same general procedure described for the synthesis of G_1-Cl. From G_3-OH (1.25 g, 0.78 mmol), $SOCl_2$ (0.13 mL, 1.75 mmol), NVP (2 mL) were obtained 1.07 g (85%) as a white solid.

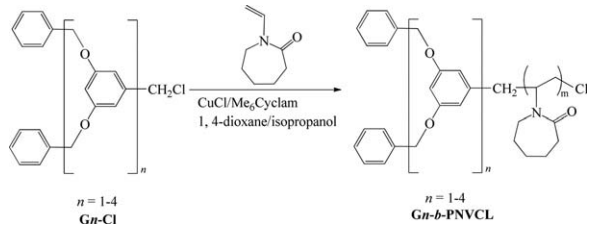

SCHEME 1 Synthesis of dendritic poly(benzyl ether)-*b*-poly(*N*-vinylcaprolactam) block copolymers (G_n-*b*-PNVCL).

^{1}H NMR (500 MHz, $CDCl_3$, δ): 4.47(s, 2H, CH_2Cl), 4.95 (s, 8H, $PhCH_2O$), 5.01 (s, 16H, $PhCH_2O$), 6.52 (m, 3H, CH), 6.55 (d, $J = 1.8$ Hz, 2H; CH), 6.64 (d, $J = 2.1$ Hz, 4H; CH), 6.66 (d, $J = 2.1$ Hz, 4H; CH), 7.27–7.40 (m, 40H, Ar H).

Synthesis of G_4-Cl

G_4-Cl was synthesized by the same general procedure described for the synthesis of G_1-Cl. From G_4-OH (0.70 g, 0.2 mmol), $SOCl_2$ (0.10 mL, 1.4 mmol), NVP (1 mL) were obtained 0.54 g (78%) as a white solid.

^{1}H NMR (500 MHz, $CDCl_3$, δ): 4.41 (s, 2H, CH_2Cl), 4.98 (s, 28H, $PhCH_2O$), 5.04 (s, 32H, $PhCH_2O$), 6.55–6.69 (m, 42H, CH), and 7.33–7.43 (m, 80H, Ar H).

Synthesis of G_n-*b*-PNVCL

The G_n-*b*-PNVCL was synthesized utilizing ATRP techniques as illustrated in Scheme 1. Typically, a Schlenk flask equipped with a magnetic stirrer was charged with NVCL (1.39g, 12.5 mmol), CuCl (0.01 g, 0.085 mmol), Me_6Cyclam (0.03 g, 0.1 mmol), a mixture of 1, 4-dioxane and isopropanol (300 μL), and pump-filled with nitrogen three times. Then the initiator G_1-Cl (0.03 g, 0.1 mmol) was added to the flask under nitrogen. The reaction mixture was stirred for 4 h. The DI water was added and stirred for 24 h. The solution was filtered off and then transferred to a dialysis bag (molecular weight cutoff = 3500) and dialyzed against deionized water for 7 days. The final product was dried in a vacuum oven, yielding a white solid.

Preparation of Micelles

In a typical procedure, a copolymer (10 mg) was dissolved in THF (3 mL). Then doubly distilled water (3 mL) was added dropwise. The solution was dialyzed against distilled water for 24 h to remove the THF. The obtained solution was transferred into a 10 mL volumetric flask, followed by dilution to the calibration mark with doubly distilled water to obtain the micellar solution of 1.0 mg mL^{-1}. The obtained micellar solution was kept for a week at room temperature, and then was filtered through a 0.45 mm-pore membrane filter before both the mean size and morphology of nanoparticles were determined by DLS and TEM, respectively. For TEM studies, a drop of micellar solution was placed onto a copper/carbon grid and the excess solution was blotted up using a strip of filter paper, and then the sample was allowed to dry at room temperature before observation.

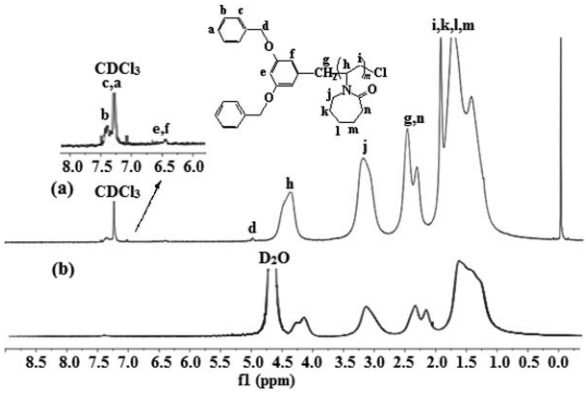

FIGURE 1 ^{1}H NMR spectra of G_1-*b*-PNVCL in $CDCl_3$ (a) and D_2O (b).

For ^{1}HNMR spectra studies, the micellar solution was prepared as above-mentioned and then freeze-dried for 48 h. The lyophilized micelles were dispersed in D_2O.

The CMC of the copolymers solution was determined with a fluorescence spectrometer (Hitachi F-4500 luminescence spectrophotometer) using pyrene as a hydrophobic probe.[42]

Temperature-Dependent Turbidimetry

The LCST of the aqueous solution of the polymer was measured at 500 nm with a UV–vis spectrometer (CARY UV-50, VARIAN) equipped with a water-circulation heating stage. The polymers were dissolved in deionized water at different concentrations (0.04–0.6 mg mL^{-1}). The heating rate was 0.2 °C min^{-1}. The LCST value was defined as the temperatures corresponding to 1% decreases of transmittance.[56]

In Vitro Cytotoxicity Testing

In vitro cytotoxicity of G_3-*b*-PNVCL and G_4-*b*-PNVCL was estimated by MTT viability assay against mouse L929 fibroblasts. L929 cells were seeded in 96 well plates at 4×10^4 cells mL^{-1} in 90 μL of Dulbecco's modified Eagle's medium (DMEM; Sigma), containing 10% fetal bovine serum, and incubated at 37 °C in a 5% CO_2 atmosphere for 24 h, followed by adding block copolymer solution (10 μL in normal saline) at different concentrations. The cells were grown for another 48 h. Then, 10 μL of MTT solution (5 mg mL^{-1}; Sigma) was added to each well. After incubating the cells for 4 h, the medium containing unreacted MTT was carefully removed. The obtained blue formazan crystals were dissolved in 100 μL per well of dissolving solution (10% sodium dodecylsulfate, 5% isobutanol, 0.012 mol L^{-1} HCl) and incubated overnight at 37 °C. Negative (normal saline) control wells were treated as above-mentioned. The absorbance at 570 and 630 nm was detected using an ELISA reader (Bio-Rad, model 680). Cell viability (as a percentage of the negative control) was calculated from the optical density values.

Immunofluorescence Microscopy

For F-actin staining, L929 cells were seeded onto glass coverslips in a 24 well plate at a density of 1×10^4 cells per well in 1mL of complete medium for 24 h after which the growth medium was removed and replaced with the medium containing three dilute solutions of G_3-*b*-PNVCL (800 μL mL^{-1}) or G_4-*b*-PNVCL (160 or 800 μg mL^{-1}), DMEM as the negative control. Then, the cells were fixed using 2% paraformaldehyde, blocked in 10% fetal calf serum at room temperature for 20 min, incubated with FITC-labeled phalloidin (1 mg mL^{-1}) for 1 h. When fixed, the cells were washed three times with PBS. The samples were imaged by fluorescence microscopy (Nikon TE2000).

RESULTS AND DISCUSSION

Synthesis and Characterization of Dendritic Poly(benzyl ether)-*b*-poly(*N*-vinylcaprolactam) Block Copolymers

Four generations of dendritic poly(benzyl ether)-*b*-poly(*N*-vinylcaprolactam) block copolymers (G_n-*b*-PNVCL) were synthesized. Scheme 1 shows the synthetic route used for the preparation of the G_n-*b*-PNVCL by ATRP of NVCL using four generations of poly(benzyl ether) dendrons having benzyl chloride focal points G_n-Cl as initiators and CuCl/Me_6Cyclam as catalyst. ^{1}H NMR, FTIR, and GPC analyses were then used to confirm the formation of G_n-*b*-PNVCL copolymers. Figures 1(a) and 2(a) as well as Supporting Information Figures S1a and S2a show the ^{1}H NMR spectra of G_n-*b*-PNVCL in $CDCl_3$. All characteristic resonances in dendritic poly(benzyl ether) blocks and PNVCL blocks can be found. The peaks at 6.55–6.58, 6.66–6.68, and 7.38 ppm [Fig. 1(a)] are attributed to the protons of dendritic poly(benzyl ether), whereas the peaks at 1.46–1.81, 3.23 and 4.41–4.51 ppm are attributed to the protons of PNVCL block. The $M_{n,\mathrm{NMR}}$ values of G_n-*b*-PNVCL were calculated based on the integration ratio of the signal at 6.55–6.58 ppm corresponding to protons e and f in the dendritic poly(benzyl ether) to that at 3.23 ppm corresponding to the methylene protons j of the PNVCL ring in the α-position to the N atom of the LDBCs. As showed in Table 1, the $M_{n,\mathrm{NMR}}$ values of the G_n-*b*-PNVCL are close to their $M_{n,\mathrm{theo}}$ values.

FTIR analysis (Supporting Information Fig. S3) of G_n-*b*-PNVCL reveals several characteristic peaks that can be correlated with the expected molecular structure of the LDBCs. The FTIR spectrum of G_1-*b*-PNVCL is shown in Supporting

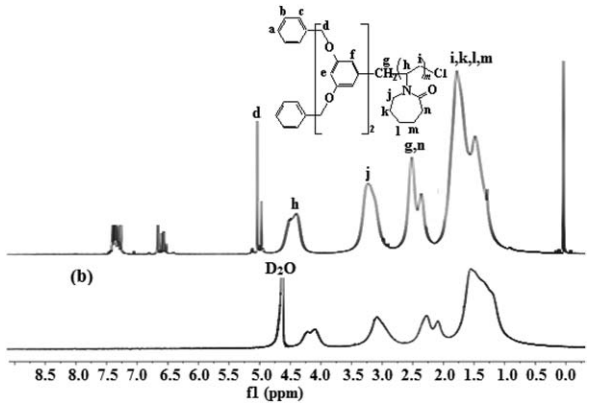

FIGURE 2 ^{1}H NMR spectra of G_2-*b*-PNVCL in $CDCl_3$ (a) and D_2O (b).

TABLE 1 Characterizations of G_n-*b*-PNVCL

Sample	$M_{n,th}$[a] (g mol^{-1})	$M_{n,GPC}$[b] (g mol^{-1})	$M_{n,NMR}$ (g mol^{-1})	PDI = M_w/M_n	Conversion (%)	DP[c]	PNVCL/dendron[d] (wt %)
G_1-*b*-PNVCL	10064.5	7757	10,126	1.02	70	71	97/3
G_2-*b*-PNVCL	9398.5	21,316	10,578	1.21	62	71	93/7
G_3-*b*-PNVCL	9969.5	22,194	11,457	1.25	60	71	87/13
G_4-*b*-PNVCL	11667.5	23,326	12,853	1.24	60	69	75/25

[a] The theoretic molecular weight was calculated by the formula: $M_{n,\,th} = M_{monomer} \times ([monomer]/[G_n\text{-Cl}]) \times Conversion\% + M_{initiation}$.
[b] M_n and PDI were determined by GPC.
[c] The degree of polymerization of PNVCL block was calculated using $M_{n,NMR}$.
[d] Dendritic poly(benzyl ether).

Information Fig. S3a as a typical example. The FTIR spectrum of G_1-*b*-PNVCL shows that the characteristic peaks at 1632 cm^{-1} for stretching vibrations of acyl group in the amide moieties of PNVCL, 1541 and 1475 cm^{-1} for the phenyl groups, 1197 cm^{-1} for C—O stretching vibration of dendritic poly(benzyl ether) were observed.

Figure 3 gave the GPC traces of G_n-*b*-PNVCL. All copolymers show unimodal GPC curves with narrow molecular weight distributions ($M_w/M_n \leq 1.25$; Table 1), which indicated that the polymerizations were controlled. However, the molecular weights from gel permeation chromatography (GPC) were not in good agreement to the targeted values as conventional calibration using linear PS standards was used.

Self-Organization in Aqueous Media of Dendritic Poly(benzyl ether)-*b*-poly(*N*-vinylcaprolactam) Block Copolymers

The presence of a hydrophobic dendritic poly(benzyl ether) and hydrophilic linear PNVCL chain means that these amphiphilic LDBCs are expected to be able to self-assemble into micelle-like nanoparticles in water. The critical micelle concentration (CMC) of amphiphilic copolymers was one of the most important parameters of characterizing the thermodynamic stability of nanoparticles in aqueous solution. Thus, the CMC of G_n-*b*-PNVCL was determined by a fluorescence technique with pyrene as a probe. The ratios of the intensity at 383–374 nm from the emission spectra of pyrene were plotted against the concentration of G_n-*b*-PNVCL. As showed in Figure 4, the I_{383}/I_{374} ratios remain fairly constant below a certain concentration and then increase remarkably above that concentration, indicating the formation of micelles. The CMC value that can be determined by intersecting the two straight lines, varied within 0.0162–0.0013 mg mL^{-1} for these LDBCs. These CMC values are comparable to those reported for some LDBCs based on flexible dendritic aliphatic polyesters which may afford additional peripheral groups used for providing functionality to the LDBCs,[57] which illustrates the effectiveness of the cone-shaped arrangement of the LDBCs and the multi-branched poly(benzyl ether) structure for improving the stability. Furthermore, it should be noted that the CMC of G_n-*b*-PNVCL decreased with increasing the generation of the dendritic poly(benzyl ether). This result demonstrated that the generation of the dendritic poly(benzyl ether) impacted the CMC of G_n-*b*-PNVCL greatly, and the high generation dendritic poly(benzyl ether) stabilized micellar aggregates due to its high hydrophobic composition.

The self-assembly of G_n-*b*-PNVCL forming micellar aggregates in aqueous was verified by ^{1}H NMR spectra. In $CDCl_3$, where micellar formation was not expected, all ^{1}H NMR resonances attributed to poly(benzyl ether) and PNVCl were detected as shown in Figures 1(a) and 2(a) and Supporting Information Fig. S1a-S2a. When the ^{1}H NMR spectra of G_n-*b*-PNVCL were recorded in D_2O, the benzyl proton peaks at 6.55–6.58, 6.66–6.68, and 7.38 ppm disappeared [Figs. 2(b) and 3(b), Supporting Information Fig. S1b-S2b], indicating that the mobility of dendritic poly(benzyl ether) segments has been

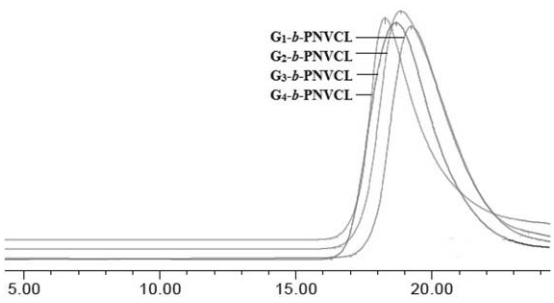

FIGURE 3 GPC traces of G_n-*b*-PNVCL.

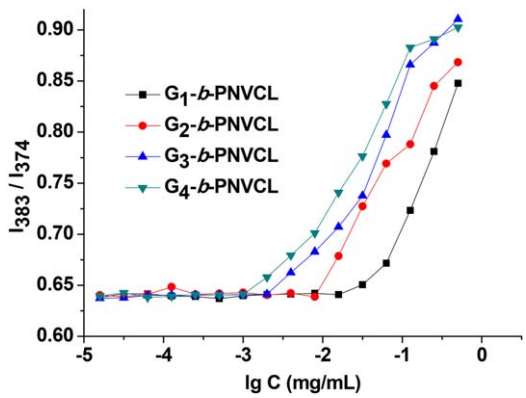

FIGURE 4 Plots of I_{383}/I_{374} versus logarithm of concentration of G_n-*b*-PNVCL. [Color figure can be viewed at wileyonlinelibrary.com]

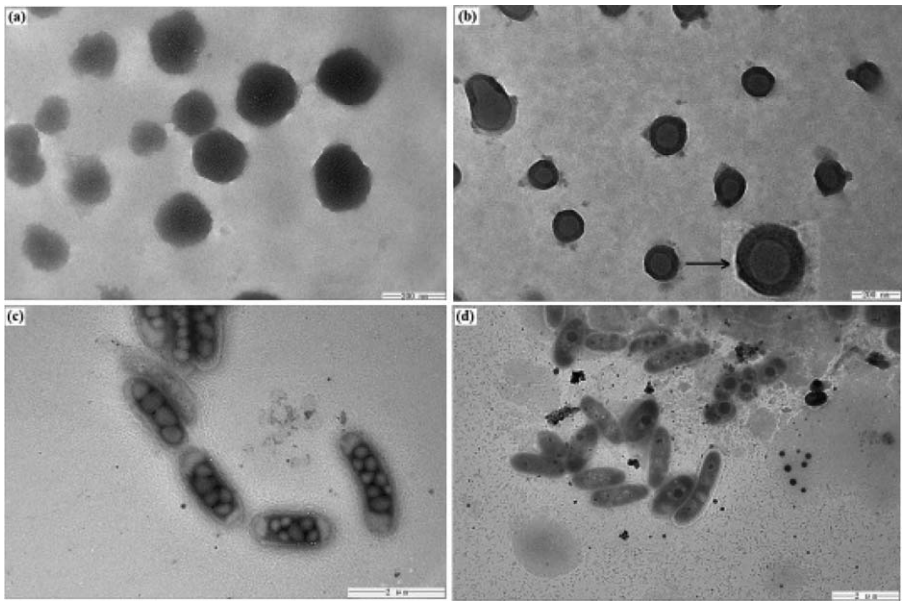

FIGURE 5 TEM images of the formed micelles by (a) G_1-*b*-PNVCL, (b) G_2-*b*-PNVCL, (c) G_3-*b*-PNVCL, and (d) G_4-*b*-PNVCL.

restricted by the formation of core-shell micellar structure in the aqueous environment.

G_n-*b*-PNVCL is first dissolved in THF, and micellization is induced by the dropwise addition of water, followed by dialysis, and the resulting dialyzed aqueous solution was subjected to an investigation of their self-assembled morphology via TEM studies. As shown in Figure 5, the multiple morphologies of the aggregates made from the LDBCs of different generations. For G_1-*b*-PNVCL, when the weight fraction of hydrophilic PNVCL block was 97 wt % within the LDBC, irregularly spherical micelles with a mean diameter of 50–130 nm were observed in Figure 5(a). However, when the weight fraction of PNVCL block decreased to 93 wt % within G_2-*b*-PNVCL, the vesicles with a mean diameter of 130–168 nm and a wall thickness of 30 nm were obtained [Fig. 5(b)]. The vesicles are dispersed very well and almost no cohesion happens during drying, which may be ascribed to the Π-Π aromatic stacking of the Fréchet-type dendrons increase the stability of the bilayer vesicle structures.[58] For G_3-*b*-PNVCL with a weight fraction of 87 wt % PNVCL, under the same self-assembly conditions, unique rod-like large compound vesicles (LCVs) are the dominant type of aggregates; 4–10 vesicles with a mean diameter of 270–560 nm aggregated together to form rod-like LCVs with tubularly packed hoops [Fig. 5(c)]. These rod-like LCVs have relatively uniform diameter (ca. 560 nm), and their lengths are in the range of 1.6–2.3 μm. Spherical or hemispherical caps are clearly seen at the rod ends. The rod-like LCVs may be ascribed to the association of individual vesicles like the intermicellar aggregation.[59] G_3-*b*-PNVCL first self-assembled into vesicles and then the vesicles further aggregated into rod-like LCVs, which most likely the length of the PNVCL block is too short to outweigh the hydrophobic-hydrophobic or van der Waals interactions between the exposed dendritic poly(benzyl ether) cores.[60] For G_4-*b*-PNVCL with a weight fraction of 75 wt % PNVCL, spherical micelles with a mean diameter of 80–150 nm as well as rod-like LCVs are obtained [Fig. 5(d)]. The size and shape of the rod-like LCVs are similar to those of LCVs from G_3-*b*-PNVCL. However, there are some smaller vesicles and spherical micelles in the rod-like LCVs, which is different from the LCVs from G_3-*b*-PNVCL. The above experimental phenomenon shows that the self-assembly behavior of G_n-*b*-PNVCL copolymers can be affected by the generation of the dendritic poly(benzyl ethers) block.

Thermoresponsive Properties of Dendritic Poly(benzyl ether)-*b*-poly(*N*-vinylcaprolactam) Block Copolymers

UV–vis spectrophotometer was first used to study the transmittances of G_n-*b*-PNVCL aqueous solution as a function of temperature with various concentrations. As shown in Figure 6, all the copolymers were transparent and colorless at the temperature below LCST (the transmittance of the solutions is close to 100%) and start to aggregate (became opaque) at LCST, which leads to a significant transition in the transmittance. The LCSTs of the copolymers G_n-*b*-PNVCL decreased in the order of G_1-*b*-PNVCL > G_2-*b*-PNVCL > G_3-*b*-PNVCL > G_4-*b*-PNVCL at all concentrations tested (Supporting Information Fig. S4), demonstrated that the generation of the LDBCs impacted the phase transition greatly, and the high generation LDBCs facilitated the collapse of the copolymers. It is well known that the LCST of thermoresponsive polymers can be adjusted by the composition of the hydrophobic and hydrophilic units. Generally, increasing hydrophobic segments leads to a decrease in the LCST of the polymer in aqueous solution and hydrophilic units had the tendency to increase LCST.[61] In this case, G_n-*b*-PNVCL copolymers possess different hydrophilic and hydrophobic compositions. The numbers of hydrophobic phenyl groups increased significantly with the generation. The high generation LDBCs

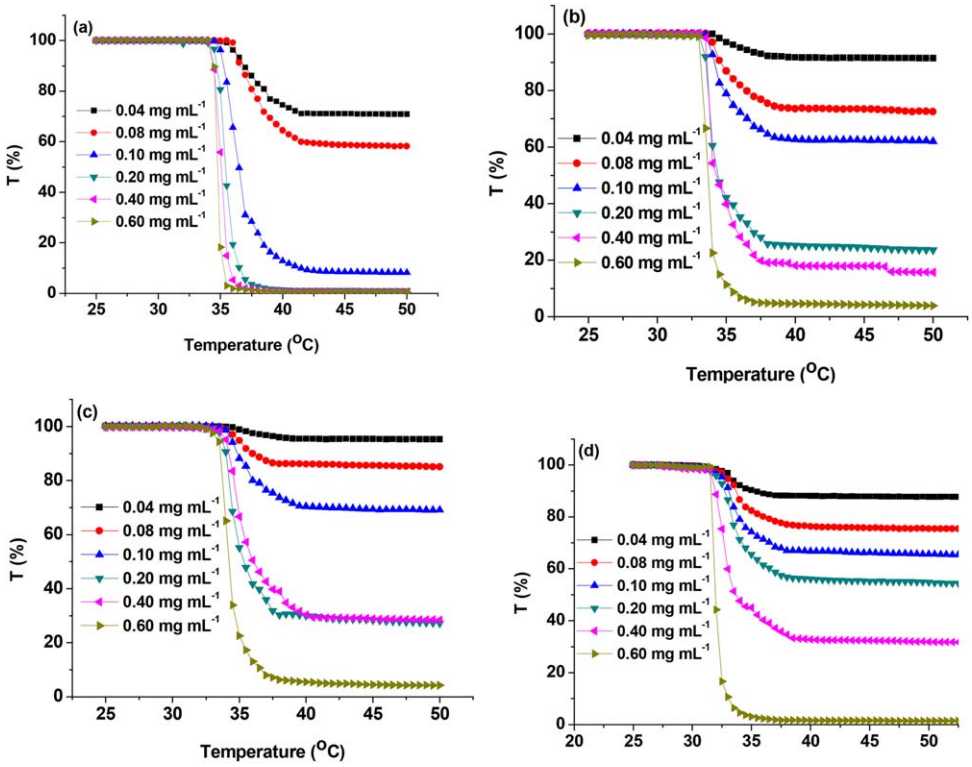

FIGURE 6 Transmittance measurements as a function of temperature for different concentrations of G_1-*b*-PNVCL (a), G_2-*b*-PNVCL (b), G_3-*b*-PNVCL (c), and G_4-*b*-PNVCL (d). [Color figure can be viewed at wileyonlinelibrary.com]

possessed more phenyl groups, which would enhance the hydrophobicity of the linear-dendritic copolymers and thus resulted in lower LCSTs. The concentration dependence of the LCSTs of these linear-dendritic copolymers was also studied. Figure 6 shows the transmittance of G_n-*b*-PNVCL as a function of temperature at different concentrations. The LCST values of G_n-*b*-PNVCL have strong concentration dependence. Their LCST values increased with decreasing the linear-dendritic copolymer concentration, and the lower the polymer concentration were, the broader the temperature range exhibited by the decrease in transmittance. Such a phenomenon is known to be a general trend in the concentration effect on the LCST of PNVCL-containing block copolymers.[38]

Jérôme and coworkers[62] noted that the transmission of poly(ethylene glycol)-*b*-poly(*N*-vinylcaprolactam) (PEG-*b*-PNVCL) block copolymers with shorter PNVCL block length cannot decrease to zero. A similar phenomenon was observed here for our linear-dendritic copolymers (Fig. 6). The remaining transmittance at high temperature is rather low (few percent) when the concentration of the copolymer was more than 0.2 mg mL^{-1} for G_1-*b*-PNVCL, 0.08 mg mL^{-1} for G_2-*b*-PNVCL, G_3-*b*-PNVCL, and G_4-*b*-PNVCL. The residual transmittance is considerable throughout (15–35%) as the concentration and generation of the linear-dendritic copolymers decrease. This phenomenon was probably attributed to the relative diminished content of thermoresponsive PNVCL segment in G_2-*b*-PNVCL, G_3-*b*-PNVCL, and G_4-*b*-PNVCL.

The thermoresponsive phase transition behavior of G_n-*b*-PNVCL copolymers was further investigated by dynamic light scattering (DLS). Figure 7 shows the temperature dependence of the average hydrodynamic radii (R_h) of the LDBCs in aqueous solution at a concentration of 1.0 mg mL^{-1} upon heating. The LCST values are in good agreement with those obtained from the turbidimetric studies and demonstrate that the LCSTs of the LDBCs depend on the generation of the dendritic poly(benzyl ethers) and decrease from 36 to 33 °C when the generation is increased from the first to fourth,

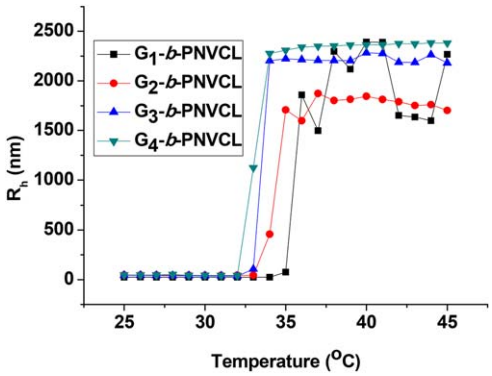

FIGURE 7 Plots of hydrodynamic radii (R_h) of the micelles formed by G_n-*b*-PNVCL in aqueous solution as a function of temperature from DLS measurements. [Color figure can be viewed at wileyonlinelibrary.com]

TABLE 2 Cell Viability Values after 48 h of Incubation with G_3-*b*-PNVCL and G_4-*b*-PNVCL at 37 °C

Concentration (μg/mL)	1.3	6.4	32	160	800
Viability (%, G_3-*b*-PNVCL)	96.1	101.7	94.4	96.7	115.0
Viability (%, G_4-*b*-PNVCL)	91.6	91.1	99.2	104.5	97.5

due to the increased the numbers of hydrophobic phenyl groups in the LDBCs.

In Vitro Cytotoxicity of Dendritic Poly(benzyl ether)-*b*-poly(*N*-vinylcaprolactam) Block Copolymers

To evaluate the biocompatibility of the obtained LDBCs, the *in vitro* cytotoxicity was measured in mouse L929 fibroblasts using the MTT assay, a valid and reliable measure of viability based on the succinic dehydrogenase activity of cultured cells. The results from the dose-response relationship for the third or fourth generation of the copolymer G_3-*b*-PNVCL or G_4-*b*-PNVCL at concentrations ranging from 1.3 to 800 μg mL^{-1} are shown in Table 2. It was demonstrated that cells remained viable even when the concentration of the LDBCs were up to 800 μg mL^{-1}, suggesting their good biocompatibility to L929 cells. The cell viabilities were >95% for G_3-*b*-PNVCL and >90% for G_4-*b*-PNVCL at the concentrations studied.

Furthermore, the F-actin staining results also demonstrate the good biocompatibility of G_3-*b*-PNVCL and G_4-*b*-PNVCL. Usually, L929 mouse fibroblasts are large, spindle-shaped, adherent cells growing as a confluent monolayer [Fig. 8(a)]. Figure 8(b–d) reflect the morphology of cells after they were cultured in a solution of G_3-*b*-PNVCL (800 μg mL^{-1}) or G_4-*b*-PNVCL (160 or 800 μg mL^{-1}) for 48 h. The dimension, shape, and density of the cells in the solution of the polymer were very similar to those in the negative control [Fig. 8(a)], indicating that no or little damage could be detected. These results demonstrate that the obtained LDBCs are potentially applicable in biomedical fields.

CONCLUSIONS

A series of new well-defined linear-dendrimeric block copolymers (LDBCs) have been synthesized in which the linear block is PNVCL and the dendrimeric block is poly(benzyl ether) of generation G_1–G_4. Their molecular structures and solution properties were characterized in detail by ^{1}H NMR, FTIR, GPC, fluorescent spectroscopy, TEM, turbidity, and DLS measurements. A morphological transition of the polymeric aggregates in water from irregularly spherical micelles, vesicles to rod-like LCVs and eventually to the coexistence of spherical micelles and rod-like LCVs has been demonstrated by increasing the generation number of the hydrophobic dendritic block. The LDBCs exhibit thermally induced phase transition in aqueous solution and their LCST decrease with increase in the generation of the dendritic poly(benzyl ethers) and the concentrations of the LDBCs solutions. The biocompatibility of the LDBCs is evaluated, and they are proven to be nontoxic to L929 cells.

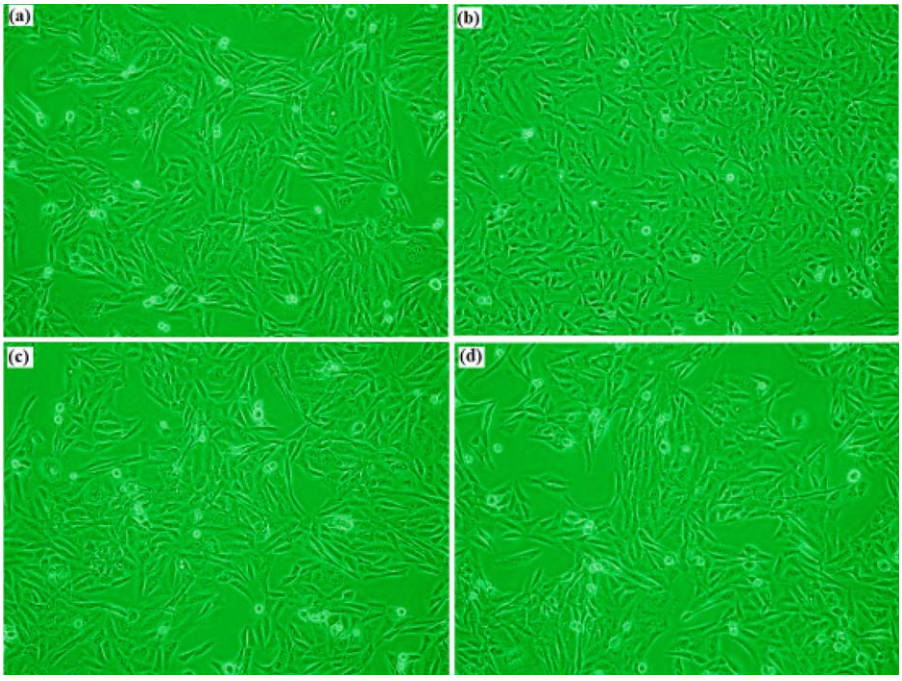

FIGURE 8 Fluorescence microscope micrographs of mouse L929 fibroblasts grown on DMEM (a), on G_3-*b*-PNVCL [b (800 μg mL^{-1})], and G_4-*b*-PNVCL [c (160 μg mL^{-1}), d (800 μg mL^{-1})] expressing F-action. [Color figure can be viewed at wileyonlinelibrary.com]

ACKNOWLEDGMENTS

The authors gratefully acknowledge support for this work of the National Natural Science Foundation of China (21264017 and 21564017).

REFERENCES AND NOTES

1 F. Wurm, H. Frey, *Prog. Polym. Sci.* **2011**, *36*, 1.

2 I. Gitsov, K. L. Wooley, J. M. J. Fréchet, *Angew. Chem. Int. Ed. Engl.* **1992**, *31*, 1200.

3 I. Gitsov, *J. Polym. Sci. Part A: Polym. Chem.* **2008**, *46*, 5295.

4 I. Gitsov, K. R. Lambrych, V. A. Remnant, R. Pracitto, *J. Polym. Sci. Part A: Polym. Chem.* **2000**, *38*, 2711.

5 A. Simonyan, I. Gitsov, *Langmuir.* **2008**, *24*, 11431.

6 G. Whitton, E. R. Gillies, *J. Polym. Sci. Part A: Polym. Chem.* **2015**, *53*, 148.

7 Z. Ge, S. Liu, *Macromol. Rapid Commun.* **2009**, *30*, 1523.

8 Y. C. Xu, C. M. Dong, *J. Polym. Sci. Part A: Polym. Chem.* **2012**, *50*, 1216.

9 Y. Yang, C. Hua, C. M. Dong, *Biomacromolecules.* **2009**, *10*, 2310.

10 C. M. Dong, G. Liu, *Polym. Chem.* **2013**, *4*, 46.

11 P. Lundberg, M. V. Walter, M. I. Montañez, D. Hult, A. Hult, A. Nyström, M. Malkoch, *Polym. Chem.* **2011**, *2*, 394.

12 Y. Li, K. Xiao, J. Luo, W. Xiao, J. S. Lee, A. M. Gonik, J. Kato, T. A. Dong, K. S. Lam, *Biomaterials.* **2011**, *32*, 6633.

13 E. Blasco, M. Piñol, L. Oriol, *Macromol. Rapid Commun.* **2014**, *35*, 1090.

14 H. Wei, S. X. Cheng, X. Z. Zhang, R. X. Zhuo, *Prog. Polym. Sci.* **2009**, *34*, 893.

15 D. Roy, W. L. A. Brooks, B. S. Sumerlin, *Chem. Soc. Rev.* **2013**, *42*, 7214.

16 S. Choi, B. Choi, C. Xue, D. Leckband, *Biomacromolecules.* **2013**, *14*, 92.

17 J. R. Gois, A. C. Serra, J. F. J. Coelho, *Eur. Polym. J.* **2016**, *81*, 224.

18 Q. Wu, D. Zhou, R. Kang, X. Tang, Q. Yang, X. Song, G. Zhang, *Chem. Asian J.* **2014**, *9*, 2850.

19 P. Shao, B. Wang, Y. Wang, J. Li, Y. Zhang, *J. Nanomater.* **2011**, *2011*, 17.

20 J. Liu, A. Debuigne, C. Detrembleur, C. Jérôme, *Adv. Healthcare Mater.* **2014**, *3*, 1941.

21 N. A. Cortez-Lemus, A. Licea-Claverie, *Prog. Polym. Sci.* **2016**, *53*, 1.

22 P. Černoch, Z. Černochová, J. Kučka, M. Hrubý, S. Petrova, P. Štěpánek, *Appl. Radiat. Isot.* **2015**, *98*, 7.

23 O. Sedlacek, B. D. Monnery, S. K. Filippov, R. Hoogenboom, M. Hruby, *Macromol. Rapid Commun.* **2012**, *33*, 1648.

24 L. Hou, P. Wu, *Soft Matter.* **2014**, *10*, 3578.

25 J. Ramos, A. Imaz, J. Forcada, *Polym. Chem.* **2012**, *3*, 852.

26 L. Liu, S. Bai, H. Yang, S. Li, J. Quan, L. Zhu, H. Nie, *Mater. Sci. Eng. C* **2016**, *67*, 581.

27 P. Singh, A. Srivastava, R. J. Kumar, *J. Polym. Sci. Part A: Polym. Chem.* **2012**, *50*, 1503.

28 X. Jiang, Y. Li, G. Lu, X. Huang, *Polym. Chem.* **2013**, *4*, 1402.

29 Y. Yang, J. Li, M. Hu, L. Chen, Y. Bi, *J. Polym. Res.* **2014**, *21*, 549.

30 D. Wan, Q. Zhou, H. Pu, G. Yang, *J. Polym. Sci. Part A: Polym. Chem.* **2008**, *46*, 3756.

31 T. Huang, X. Wang, T. Malmgren, K. Hong, J. W. Mays, *Macromol. Chem. Phys.* **2012**, *213*, 2450.

32 M. Beija, J. D. Marty, M. Destara, *Chem. Commun.* **2011**, *47*, 2826.

33 L. Shao, M. Hu, L. Chen, L. Xu, Y. Bi, *React. Funct. Polym.* **2012**, *72*, 407.

34 Y. C. Yu, G. Li, J. Kim, J. H. Youk, *Polymer.* **2013**, *54*, 6119.

35 M. Hurtgen, J. Liu, A. Debuigne, C. Jérôme, C. Detrembleur, *J. Polym. Sci. Part A: Polym. Chem.* **2012**, *50*, 400.

36 J. M. Thomassin, K. Mathieu, A. Kermagoret, C. A. Fustin, C. Jérôme, A. Debuigne, *Polym. Chem.* **2015**, *6*, 1856.

37 A. Kermagoret, C. A. Fustin, M. Bourguignon, C. Detrembleur, C. Jérôme, A. Debuigne, *Polym. Chem.* **2013**, *4*, 2575.

38 Y. Yang, G. Tang, M. Hu, L. Shao, J. Li, Y. Bi, *Polymer.* **2015**, *68*, 213.

39 G. D. García-Olaiz, K. A. Montoya-Villegas, A. Licea-Claverie, N. A. Cortez-Lemus, *React. Funct. Polym.* **2015**, *88*, 16.

40 T. Cai, M. Li, B. Zhang, K. Neoh, E. Kang, *J. Mater. Chem. B.* **2014**, *2*, 814.

41 Y. Bi, C. Yan, L. Shao, Y. Wang, Y. Ma, G. Tang, *J. Polym. Sci. Part A: Polym. Chem.* **2013**, *51*, 3240.

42 G. Tang, M. Hu, Y. Ma, D. You, Y. Bi, *RSC Adv.* **2016**, *6*, 42786.

43 N. A. Cortez-Lemus, A. Licea-Claverie, *J. Polym. Sci. Part A: Polym. Chem.* **2016**, *54*, 2156.

44 M. R. Leduc, C. J. Hawker, J. Dao, J. M. J. Fréchet, *J. Am. Chem. Soc.* **1996**, *118*, 11111.

45 M. R. Leduc, W. Hayes, J. M. J. Fréchet, *J. Polym. Sci. Part A: Polym. Chem.* **1998**, *36*, 1.

46 I. Gitsov, C. Zhu, *J. Am. Chem. Soc.* **2003**, *125*, 11228.

47 I. Gitsov, A. Simonyan, N. G. Vladimirov, *J. Polym. Sci. Part A: Polym. Chem.* **2007**, *45*, 5136.

48 M. Adeli, Z. Zarnegar, A. Dadkhah, R. Hossieni, F. Salimi, A. Kanani, *J. Appl. Polym. Sci.* **2007**, *104*, 267.

49 Z. Shi, H. Lu, Z. Chen, R. Cheng, D. Chen, *Polymer.* **2012**, *53*, 359.

50 J. del Barrio, L. Oriol, C. Sánchez, J. L. Serrano, A. Di Cicco, P. Keller, M.-H. Li, *J. Am. Chem. Soc.* **2010**, *132*, 3762.

51 R. Jevprasesphant, J. Penny, R. Jalal, D. Attwood, N. B. McKeown, A. D'Emanuele, *Int. J. Pharm.* **2003**, *252*, 263.

52 R. Duncan, L. Izzo, *Adv. Drug Delivery Rev.* **2005**, *57*, 2215.

53 R. W. Hay, G. A. Lawrance, N. F. Curtis, *J. Chem. Soc. Perkin Trans.* **1975**, *1*, 591.

54 C. J. Hawker, J. M. J. Fréchet, *J. Am. Chem. Soc.* **1990**, *112*, 7638.

55 N. Yamazaki, I. Washio, Y. Shibasaki, M. Ueda, *Org. Lett.* **2006**, *8*, 2321.

56 J. Xu, J. Ye, S. Liu, *Macromolecules.* **2007**, *40*, 9103.

57 E. R. Gillies, T. B. Jonsson, J. M. J. Fréchet, *J. Am. Chem. Soc.* **2004**, *126*, 11936.

58 D. Xie, M. Jiang, G. Zhang, D. Chen, *Chem. Eur. J.* **2007**, *13*, 3346.

59 C. Allen, Y. Yu, D. Maysinger, A. Eisenberg, *Bioconjugate Chem.* **1998**, *9*, 564.

60 Y. Chang, C. Park, K. T. Kim, C. Kim, *Langmuir.* **2005**, *21*, 4334.

61 H. Feil, Y. H. Bae, J. Feijen, S. W. Kim, *Macromolecules.* **1993**, *26*, 2496.

62 J. Liu, C. Detrembleur, M. C. De Pauw-Gillet, S. Mornet, E. Duguet, C. Jérôme, *Polym. Chem.* **2014**, *5*, 799.